Shell-to-shell energy transfer in magnetohydrodynamics. II. Kinematic dynamo

Pablo Mininni,* Alexandros Alexakis,† and Annick Pouquet
National Center for Atmospheric Research, P.O. Box 3000, Boulder, Colorado 80307, USA
(Received 19 May 2005; published 4 October 2005)

We study the transfer of energy between different scales for forced three-dimensional magnetohydrodynamics turbulent flows in the kinematic dynamo regime. Two different forces are examined: a nonhelical Taylor-Green flow with magnetic Prandtl number $P_M=0.4$ and a helical ABC flow with $P_M=1$. This analysis allows us to examine which scales of the velocity flow are responsible for dynamo action and identify which scales of the magnetic field receive energy directly from the velocity field and which scales receive magnetic energy through the cascade of the magnetic field from large to small scales. Our results show that the turbulent velocity fluctuations in the inertial range are responsible for the magnetic field amplification at small scales (small-scale dynamo) while the large-scale field is amplified mostly due to the large-scale flow. A direct cascade of the magnetic field energy from large to small scales is also presented and is a complementary mechanism for the increase of the magnetic field at small scales. The input of energy from the inertial range velocity field into the small magnetic scales dominates over the energy cascade up to the wave number where the magnetic energy spectrum peaks. At even smaller scales, most of the magnetic energy input is from the cascading process.

DOI: 10.1103/PhysRevE.72.046302 PACS number(s): 47.65.+a, 47.27.Gs, 95.30.Qd

I. INTRODUCTION

Dynamo action is often invoked to explain the generation and sustainment of magnetic fields in astronomical objects. In the magnetohydrodynamics (MHD) dynamo, an initially small magnetic field is amplified by currents induced solely by the motion of a conducting fluid [1]. In typical astrophysical situations where amplified magnetic fields are met, the velocity field is composed of a large-scale flow (e.g., rotation and/or meridional flows) together with turbulent fluctuations in smaller scales. As an example, in the Sun both large- and small-scale magnetic fields are observed. The large-scale components of the magnetic field are generated by a large-scale flow [2]. Simulations also show that the small-scale magnetic fields can be generated by turbulent fluctuations in the convective region [3]. Understanding the generation of magnetic fields under these conditions and the role played by the two components of the flow (large scale and turbulent) is today a crucial aspect of dynamo theory.

Dynamos are often classified as small-scale and large-scale dynamos, depending on the properties of the amplified magnetic field [4]. In large-scale dynamos, the focus is on whether a flow can amplify and sustain magnetic fields at scales larger than the velocity integral scale. This interest is motivated by astrophysical problems where large-scale magnetic fields are actually observed, such as the dipolar component in stars and planets. The amplification of the magnetic field in these scales is usually explained by invoking a turbulent α effect and/or amplification due to a large-scale flow. The linear (or kinematic) regime of large-scale dynamo action has been studied with the use of mean-field theory [5,6] and MHD closures [7] and with the aid of numerous direct numerical simulations (DNS's) (see, e.g., [8–10]). In theoretical investigations of large-scale dynamo action, helical flows are generally considered, which are thought of as better candidates for amplifying the magnetic field at larger scales. However, the presence of helicity is not necessarily needed to generate large-scale magnetic fields [11]; they can also be amplified in nonhelical flows if anisotropy [12] or other mean-field effects [13,14] are present.

Small-scale dynamos, on the other hand, amplify magnetic fields on scales smaller than the energy containing scales of the turbulence [15–19]. Theoretical investigations usually involve assumptions of nonhelical velocity fields (see, however, [20]), δ correlated in time (as a simplifying approximation to a turbulent flow), and often the limit of large magnetic Prandtl number $P_M>1$ is considered. Numerically small-scale dynamos have been investigated in Refs. [8,18,19]. Here we note that an argument due to Batchelor [21] suggests that this dynamo can only operate if $P_M>1$. However, there are reasons to believe the small-scale dynamo can work even when $P_M<1$ if the magnetic Reynolds number R_M is large enough [22,23].

However, this separation between large-scale and small-scale dynamos is in some cases artificial and may be misleading. Most astronomical objects display a large-scale flow with turbulent fluctuations at smaller scales, and both large- and small-scale magnetic fields are observed. The transition between the two magnetic fields is often smooth, and a clear distinction between the two cannot be made. This has led some authors to develop models trying to unify the two regimes [24]. Furthermore, the two amplification mechanisms in the small and large scales are coupled in many cases and cannot be considered independently. According to mean-field theory [6,16], the large-scale magnetic field in a turbulent dynamo results from the small-scale (helical) velocity fields. Moreover, concerning the amplification of small-scale magnetic fields, it has been argued that when a large-scale magnetic field is present, small scales can be generated by the

*Electronic address: mininni@ucar.edu
†Electronic address: alexakis@ucar.edu

distortion of large-scale field lines (see, e.g., [1]), even in the absence of self-excitation (small-scale dynamo action). This is a common assumption in mean-field dynamos, where it is often considered that the needed small-scale magnetic fields are only fed by the large-scale field through a nonlinear cascade process.

In the presence of both a large-scale flow and turbulent fluctuations, the role played by the different scales involved in the amplification process is thus of crucial importance and is not well understood. When magnetic fields are present at scales both smaller and larger than the energy containing scales of the velocity field, it is not clear what portion of the small-scale magnetic field is generated by direct cascade of magnetic energy from the large scales and what from self-excitation. Furthermore, it is not well understood what portion of the amplification of the large- or small-scale dynamo is due to the forced component of the flow and what part is due to the turbulent fluctuations which emerge through nonlinear interactions at high Reynolds number. To answer these questions, a detailed study of the energy transfer from the different velocity scales to the different magnetic scales is required. This kind of approach naturally raises the question of the locality (in Fourier space) of the interactions that are taking place in a turbulent dynamo.

In a companion paper [25] (hereafter referred to as paper I), the transfer of energy between the velocity and magnetic field at different scales was studied for mechanically forced MHD turbulence in a steady state where both fields are in quasiequipartition by introducing the energy transfer functions between different shells of wave numbers in Fourier space (see also [26,27]). In this paper, we present shell-to-shell energy transfers during the kinematic regime of two different MHD dynamos. Our main interest is to identify which velocity field scales are responsible for the amplification of the large- and small-scale magnetic field, which scales of the magnetic field receive most of the energy, and how the magnetic energy cascades among the different scales.

In Sec. II we present a brief review of the equations and definition of transfer functions needed to study this problem, and in Sec. III we give the results from simulations; we also discuss in this section some details of the nonlinear saturation of the dynamo. Finally, in Sec. IV we present the conclusions of our work.

II. TRANSFER FUNCTIONS

We will consider the incompressible MHD equations

$$\partial_t \mathbf{u} + \mathbf{u}\cdot\nabla\mathbf{u} = -\nabla p + \mathbf{b}\cdot\nabla\mathbf{b} + \nu\nabla^2\mathbf{u} + \mathbf{f}, \tag{1}$$

$$\partial_t \mathbf{b} + \mathbf{u}\cdot\nabla\mathbf{b} = \mathbf{b}\cdot\nabla\mathbf{u} + \eta\nabla^2\mathbf{b}, \tag{2}$$

where $\mathbf{u}$ is the velocity field, $\mathbf{b}$ is the magnetic field, ν is the kinematic viscosity, η is the magnetic diffusivity, p is the total pressure, and $\mathbf{f}$ a constant external force. These equations are accompanied by the conditions $\nabla\cdot\mathbf{u}=0=\nabla\cdot\mathbf{b}$. Equations (1) and (2) are solved in a periodic domain using a pseudospectral method with the 2/3 dealiasing rule and second-order Runge-Kutta method to advance in time.

We are interested in the kinematic regime of the dynamo, where a small magnetic seed is amplified exponentially without modifying the velocity field (i.e., the effect of the Lorentz force on the velocity field is negligible).

To this end, we made two numerical simulations using a grid of 256^3 points under the following procedure. First, a hydrodynamic simulation was performed to obtain a turbulent steady state. Then, a random small magnetic field was introduced and the simulation was carried, keeping the force fixed to observe exponential amplification of the magnetic energy. The data were analyzed during this stage and as the systems approached saturation.

Two expressions for the external force were used: Taylor-Green (TG) and ABC. The TG forcing is nonhelical ($\mathbf{f}\cdot\nabla\times\mathbf{f}=0$ pointwise), while the ABC forcing is of maximum helicity and the resulting flow has non-negligible helicity (for a description of the resulting flows see, e.g., [28,29]). In both simulations, the amplitude of the external force was set to obtain a unity rms velocity, and the characteristic wave number of the force was chosen to obtain a large scale flow at $k_F\sim 3$. The TG simulation had $\nu=2\times10^{-3}$ and $\eta=5\times10^{-3}$ (the magnetic Prandtl number in this simulation was $P_M=\nu/\eta=0.4$). In the ABC run, $\nu=\eta=2\times10^{-3}$ ($P_M=1$). The mechanical Reynolds numbers reached by the two flows are Re=675 for the Taylor-Green flow and Re=820 for the ABC [28,29].

As we stated in the Introduction, we are interested in quantifying the rate of energy transfer from the different scales of the velocity field to the different scales of the magnetic field. To rigorously define the velocity and magnetic field at different scales we introduce the shell-filtered velocity and magnetic field components $\mathbf{u}_K(\mathbf{x})$ and $\mathbf{b}_K(\mathbf{x})$, where the subscript K indicates that the field has been filtered to keep only the modes in the Fourier shell $[K,K+1)$ (hereafter called shell K). Clearly the sum of all K components gives back the original field. We are interested therefore in the rate that energy from the velocity or magnetic field at a given shell Q is transferred into kinetic or magnetic energy at another shell K. From the MHD equations, taking the dot product of Eq. (2) with $\mathbf{b}_K$ and integrating over space, we obtain the evolution of the magnetic energy $E_b(K)=\int b_K^2/2dx^3$ in shell K:

$$\partial_t E_b(K) = \sum_Q [\mathcal{T}_{ub}(Q,K) + \mathcal{T}_{bb}(Q,K)] - \eta\mathcal{D}_b(K), \tag{3}$$

where we have introduced the two transfer functions $\mathcal{T}_{ub}(Q,K)$ and $\mathcal{T}_{bb}(Q,K)$ as defined below. The transfer rate of kinetic energy at shell Q into magnetic energy at shell K is defined as

$$\mathcal{T}_{ub}(Q,K) = \int \mathbf{b}_K(\mathbf{b}\cdot\nabla)\mathbf{u}_Q d\mathbf{x}^3, \tag{4}$$

and the transfer rate of magnetic energy from shell Q into shell K is defined as

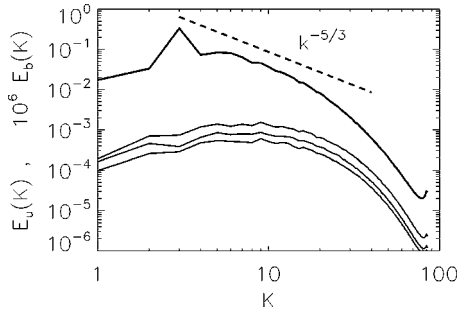

FIG. 1. Spectra of kinetic energy (thick solid line) and magnetic energy (thin solid line) scaled up by a factor 10^6 for the Taylor-Green runs during the kinematic dynamo regime. The dashed line indicates the Kolmogorov slope as a reference. Note that during this stage, all the magnetic modes grow with approximately the same rate.

$$\mathcal{T}_{bb}(Q,K) = -\int \mathbf{b}_K(\mathbf{u}\cdot\boldsymbol{\nabla})\mathbf{b}_Q d\mathbf{x}^3. \tag{5}$$

The transfer $\mathcal{T}_{ub}(Q,K)$ is due to the stretching of magnetic field lines by the velocity field gradients and leads to energy input in the magnetic field. This term is responsible for dynamo action—i.e., conversion of kinetic energy into magnetic energy. The function $\mathcal{T}_{bb}(Q,K)$ is due to the advection of magnetic field vector components by the velocity field, and it does not amplify the total magnetic energy. Instead, it is responsible for the redistribution of magnetic energy among the different shells and it is related to the cascade of magnetic energy from larger to smaller scales. Finally, we introduced the dissipation rate $\mathcal{D}_b(K)$ in shell K defined as

$$\mathcal{D}_b(K) = -\int |\boldsymbol{\nabla}\times\mathbf{b}_K|^2 d\mathbf{x}.$$

More detailed definitions of these transfer terms and their general properties can be found in paper I.

We measured the transfer functions based on Eqs. (4) and (5) using ten different outputs (corresponding to ten different times) for each run during the kinematic regime. The transfers were normalized using the total magnetic energy and were then averaged. As the system was approaching saturation and was deviating from the exponential growth, single-time outputs were used and the transfer functions were normalized using the total magnetic energy, but were not averaged, since in this stage the normalized magnetic energy spectrum is changing with time. From here on, we will use the notations $\mathcal{T}_{ub}(Q,K)$ and $\mathcal{T}_{bb}(Q,K)$ for the normalized transfer functions $\mathcal{T}_{ub}(Q,K)/\Sigma_{K'}E_b(K')$ and $\mathcal{T}_{bb}(Q,K)/\Sigma_{K'}E_b(K')$, unless otherwise noted.

III. RESULTS

A. Kinematic regime

We begin by describing the general properties of the two dynamos investigated in this work. Figure 1 shows the kinetic and magnetic energy spectra for a TG simulation in the kinematic dynamo regime. In Fig. 2 we show the same spectra for the ABC run. Note that the kinetic energy spectrum peaks in both cases at $k_F \sim 3$, where a well-defined large-scale flow is present. For larger wave numbers the spectrum has a short inertial range, with Kolmogorov scaling. During the kinematic regime, the magnetic energy spectrum peaks at small scales ($k \sim 9$ for TG and $k \sim 12$ for ABC) and all the modes grow exponentially with the same rate. As a result, all the spectra (and transfer functions) preserve their dependence with wave number (up to an amplitude normalization) as time evolves.

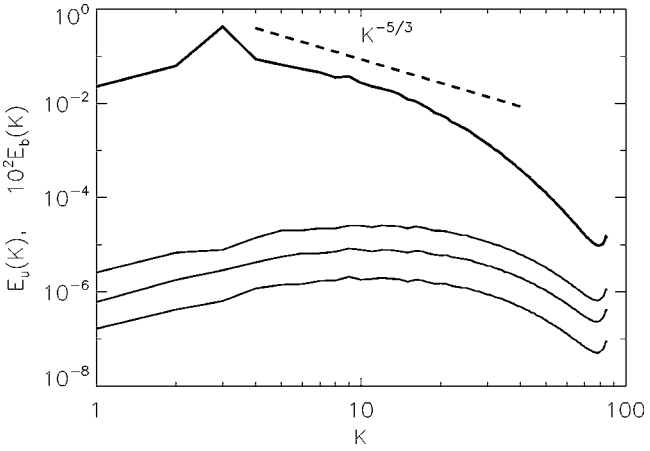

FIG. 2. Spectra of kinetic energy (thick solid line) and magnetic energy (thin solid line) scaled up by a factor 10^2 for the ABC runs. The dashed line indicates the Kolmogorov slope as a reference.

To study the kinematic regime, the MHD simulations were started with a random magnetic field with values of magnetic energy as low as $E_M/E_K = 5\times10^{-9}$ to ensure that the Lorentz force was negligible at all wave numbers even with the magnetic energy spectrum peaking at small scales.

We first start with some general properties of the two transfer functions. Contour plots of the transfers $\mathcal{T}_{ub}(Q,K)$ and $\mathcal{T}_{bb}(Q,K)$ during the kinematic regime of the TG run are shown in Fig. 3. The gray scale indicates magnitude of the transfer, with "dark" being positive and "bright" negative. The figure should be interpreted as follows: At a given point (Q,K) in Fig. 3(a), where the transfer is positive (negative), energy is given (received) by the velocity field at the scale Q to (from) the magnetic field at scale K. Similarly at a given point (Q,K) in Fig. 3(b), where the transfer is positive (negative), energy is given (received) by the magnetic field at the scale Q to the magnetic field at scale K.

Note that $\mathcal{T}_{bb}$ is by definition antisymmetric along the diagonal $K=Q$ and is mostly concentrated in the surroundings of the diagonal. The $\mathcal{T}_{ub}$ transfer is concentrated on a triangle below the diagonal and is positive everywhere. The fact that $\mathcal{T}_{bb}$ is concentrated along the diagonal implies, as we will show later, locality of interactions, while the "triangular" shape of $\mathcal{T}_{ub}$ implies long-range interactions in Fourier space.

To draw conclusions from the functional form of the transfers we need to examine their behavior for different fixed values of K or Q. Figures 4 and 5 show the $\mathcal{T}_{ub}(Q,K)$ function at constant values of Q for the TG and ABC simulations, respectively. The transfer is always positive, implying that kinetic energy is transferred from all velocity wave

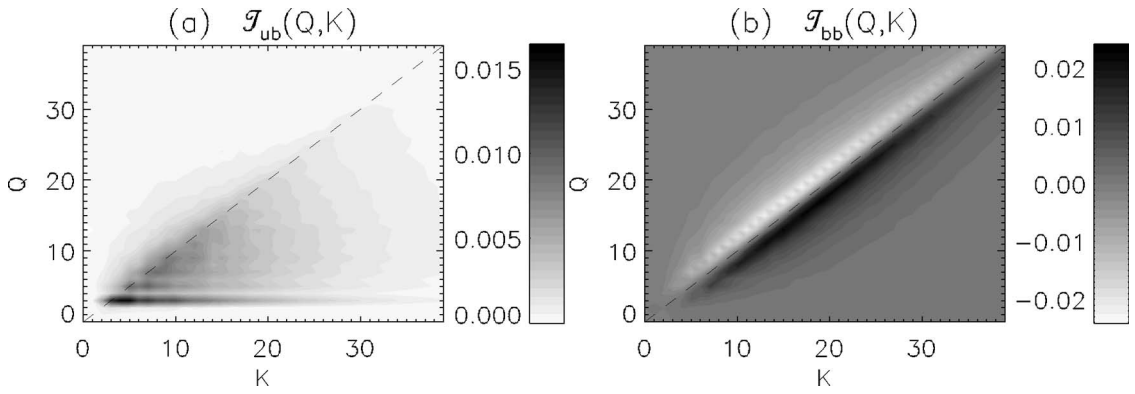

FIG. 3. Transfer functions (a) $\mathcal{T}_{ub}$, and (b) $\mathcal{T}_{bb}$ [see Eqs. (4) and (5)] as a function of Q and K in the TG run during the kinematic regime. $\mathcal{T}_{ub}$ is positive for all values of Q and K shown. Each point (Q,K) in panel (a) represents the rate of transfer of energy from velocity mode Q to magnetic mode K. Each point (Q,K) in panel (b) represents the rate of transfer of energy from magnetic mode Q to magnetic mode K. The dashed line indicates the diagonal $K=Q$.

numbers Q to magnetic energy at different K shells. The transfer is maximum for wave numbers close to Q and then slowly decays. Note that in the ABC run the flow at $Q=3$ gives more energy than the turbulent fluctuations ($Q=5,10,20,30$) when compared with the TG simulation. This is related to the fact that in the ABC run the $Q=3$ shell contains most of the kinetic helicity of the flow, an ingredient known to be relevant for dynamo action [1,6]. We note here that since the transfers are normalized by the total magnetic energy and the two runs have different magnetic energy spectra, a direct comparison of the values of the transfers between the two runs cannot be made.

In Figs. 6 and 7 we show the same transfer function $\mathcal{T}_{ub}$ but now for constant values of K. The transfer is positive at all scales, pointing to the fact that all velocity shells are giving energy to the magnetic field (compare this result with the turbulent steady state in paper I, where energy is being transferred from the magnetic field to the velocity field at small scales). A peak at $Q=3$ can be identified at all wave numbers K, indicating that the large-scale flow gives energy nonlocally to all magnetic shells. For wave numbers $Q>3$ also a plateau can be identified, where $\mathcal{T}_{ub}$ as a function of Q is approximately constant. The plateau drops at $K \gtrsim Q$. This region of constant $\mathcal{T}_{ub}$ corresponds to all kinetic energy shells at $3<Q\lesssim K$ (the turbulent fluctuations) transferring the same amount of energy to the magnetic field at shell K. In the ABC simulations, the role played by the turbulent fluctuations is again observed to be smaller than in the TG runs when compared with the large-scale flow at $Q\sim 3$.

The transfer of magnetic energy between different scales is shown in Fig. 8. As previously mentioned, this transfer is associated with the cascade of energy to smaller scales. Each shell Q is giving energy to a slightly larger wave number K (the positive peak of the curves) and receiving energy from a slightly smaller wave number K' (the negative peak of the curves). There is an increase of the amplitude of the transfer as the wave number Q is increased up until the peak of the spectrum is reached and then it drops again. This transfer function drops fast for wave numbers K and Q far apart and therefore indicates a local transfer of energy.

We are ready now to answer some of the questions posed in the Introduction. First we want to consider if it is the large-scale flow that drives the dynamo or the turbulent fluctuations. On average the contribution to the injection of magnetic energy from the large-scale flow is 16% for the TG flow and 25% for the ABC flow. Note that this fraction is much smaller than what is obtained in the saturated regime (60% for TG and 75% for ABC in [25]). Furthermore, the influence of the large-scale flow becomes smaller as we are deeper in the inertial range. In Fig. 9 we show the ratio

$$\mathcal{R}_{LS}(K) = \sum_{Q=2,3,4} \mathcal{T}_{ub}(Q,K) \Big/ \sum_{Q} \mathcal{T}_{ub}(Q,K),$$

which expresses the fraction of energy a magnetic shell K receives only from the the large-scale flow (the peak at Q

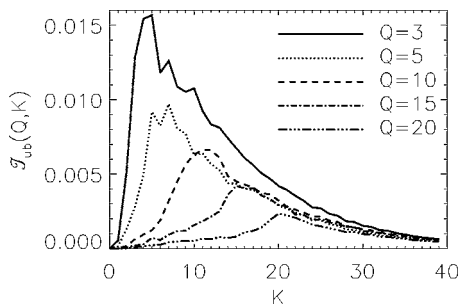

FIG. 4. Transfer function $\mathcal{T}_{ub}(Q,K)$ (from the kinetic energy at Q to the magnetic energy at K) for fixed values of Q during the kinematic regime of the TG run.

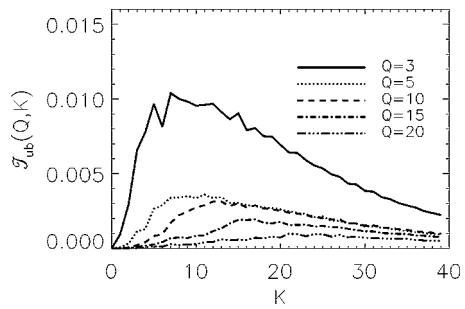

FIG. 5. Transfer function $\mathcal{T}_{ub}(Q,K)$ for fixed values of Q during the kinematic regime of the ABC run.

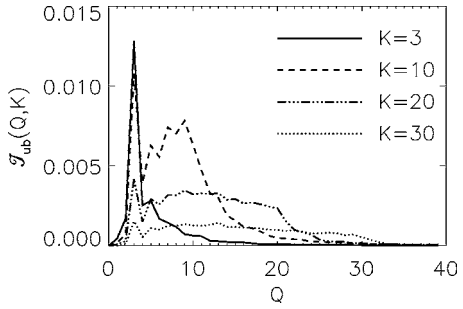

FIG. 6. Transfer function $\mathcal{T}_{ub}(Q,K)$ for fixed values of K during the kinematic regime of the TG run.

$=2,3,4$ in Figs. 6 and 7) to the total energy received by the same shell from the velocity field at all scales. For both flows the energy input from large scales becomes smaller as the wave number K is increased and the large-scale flow only dominates the injection of magnetic energy over a small range $K_F<K<K_{LS}$, with $K_{LS}\simeq 5$. This indicates that for large Reynolds numbers and in scales much smaller than the forced scales the input of energy directly from the large-scale flow is not as important.

Another question we posed in the Introduction is whether the small-scale magnetic fluctuations are the result of a cascade of energy from the large-scale magnetic field or from a direct input of energy (amplification) from the velocity field. To answer this question, in Fig. 9 we also plot the ratio

$$\mathcal{R}_C(K) = \sum_{Q=0}^{K} \mathcal{T}_{bb}(Q,K) \Big/ \sum_{Q} \mathcal{T}_{ub}(Q,K),$$

which expresses the fraction of energy a magnetic shell K receives from the cascade of energy from larger magnetic scales to the total energy received in the same shell directly from the velocity field. The cascading term appears to be smaller up to a wave number $K_C\simeq 12$ close to the peak of the magnetic energy spectrum. For $K>K_C$ there is more energy input from the cascade than the input from the velocity field. Between these two processes, a range of wave numbers $K_{LS}<K<K_C$ exists where the amplification of the magnetic field is purely dominated by injection from the turbulent velocity scales. Note that the existence of these three different regions in Fourier space and the values of the wave numbers

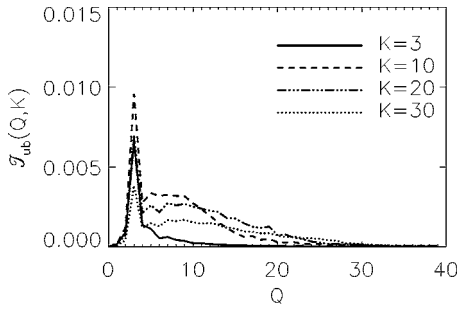

FIG. 7. Transfer function $\mathcal{T}_{ub}(Q,K)$ for fixed values of K during the kinematic regime of the ABC run.

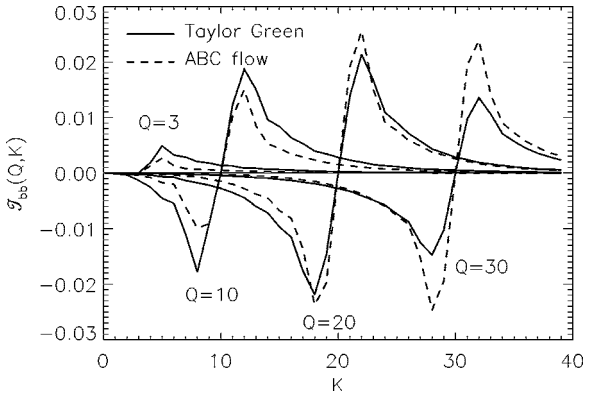

FIG. 8. Transfer function $\mathcal{T}_{bb}(Q,K)$ (from magnetic energy at shell Q to magnetic energy at shell K) at fixed values of Q during the kinematic regime of the TG and ABC runs.

K_{LS} and K_C can be expected to depend on the values of the Reynolds numbers.

We also investigate the growth rate of large-scale magnetic fields restricted to the shells $K=1,2$. In order to obtain the highest possible Reynolds numbers in the simulations, the scale separation between the forcing band and the large-scale magnetic field was chosen to be small, and therefore an investigation of the α dynamo effect is not possible in the present study. Here we just limit ourselves to investigate which scale of the velocity field is responsible for the input of energy in the large scales $K=1$ and $K=2$ of the magnetic field. In Fig. 10 we show the transfer of energy from the velocity field to these large-scale modes. Although there is a contribution from the turbulent fluctuations, the bulk of the energy originates from the forced modes. A similar result was obtained in Ref. [9], in simulations with larger-scale separation ($k_F\simeq 5$) but lower Reynolds numbers.

Finally, in both simulations, all wave numbers are observed to grow with the same growth rate during the kinematic regime. To investigate this we can write the energy

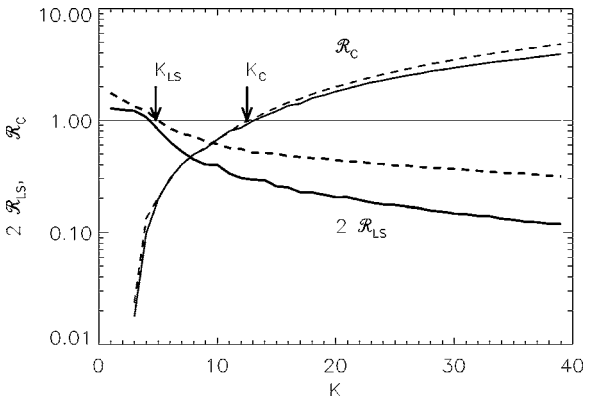

FIG. 9. Ratio $\mathcal{R}_{LS}$ of energy received by the magnetic field at wave number K from the forced wave numbers against all wave numbers and ratio $\mathcal{R}_C$ of energy received by the magnetic field at wave number K from the magnetic field at larger scales through a cascade process against energy received from the velocity field. The solid lines correspond to the TG run while the dashed lines correspond to the ABC run, both in the kinematic regime.

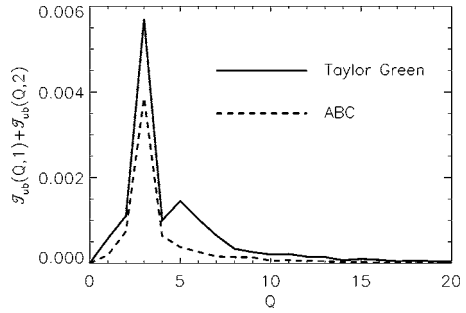

FIG. 10. Energy received by the magnetic field at scales larger than the forcing band ($K=1$ and 2) from the velocity field at wave numbers Q.

budget using the induction equation (2) in Fourier space. Taking the dot product with the magnetic field $\mathbf{b}_K$ at shell K and dividing by the magnetic energy $E_b(K)$ in that shell, we finally obtain

$$\frac{1}{E_b(K)}\frac{\partial}{\partial t}E_b(K) = \frac{1}{E_b(K)}\sum_Q [\mathcal{T}_{ub}(Q,K) + \mathcal{T}_{bb}(Q,K)] - \eta K^2, \tag{6}$$

where the simplification $\mathcal{D}(K) \simeq K^2 E_b(K)$ was used. The left-hand side of Eq. (6) gives the growth rate σ. The first two terms on the right-hand side are the energy received by the magnetic field at shell K from the velocity field and from the magnetic field at all scales. The last term is the Ohmic dissipation. In Figs. 11 and 12 we show each term of this budget as a function of the wave number K for the TG and ABC runs. The difference between the solid line and the dotted line is the growth rate. In spite of the fluctuations, the growth rate seems to be constant in a wide range of wave numbers. This is more clearly observed in the ABC run because of the larger growth rate in this simulation. The constant growth

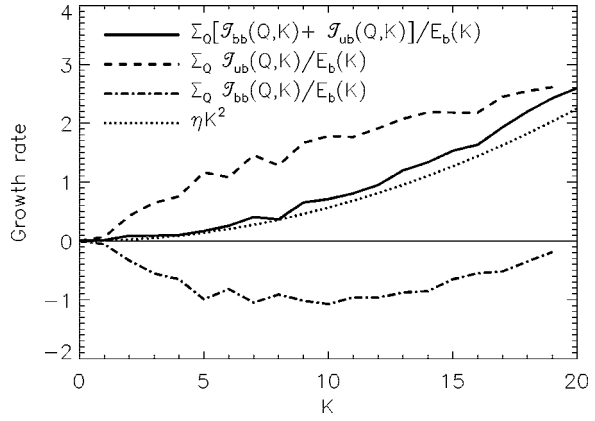

FIG. 11. Terms determining the growth rate of magnetic energy [see Eq. (6)] as a function of wave number K for the TG run during the kinematic regime. The dashed line is the energy received by the magnetic field from the velocity field, and the dash-dotted line is the cascade of magnetic energy. The solid line is the total energy received by the magnetic field, while the dotted line is the Ohmic dissipation. The difference between the last two curves gives the growth rate.

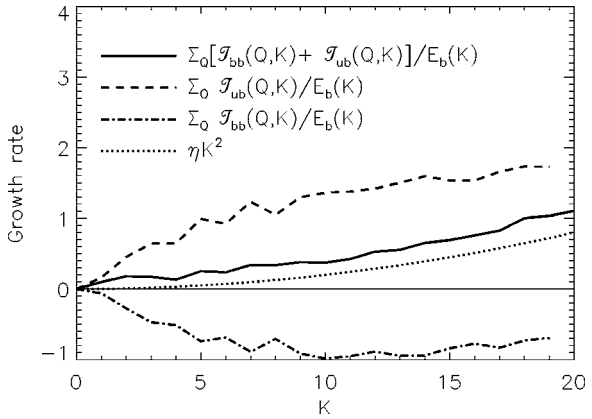

FIG. 12. The budget of magnetic energy giving rise to the growth rate for the ABC run during the kinematic regime. Labels are as in Fig. 11.

rate over all scales therefore is the result of a balance between the energy received by the magnetic field at each shell K locally (from the direct cascade), nonlocally (from the stretching of field lines), and of the Ohmic dissipation. Note that when integrated over all Q, the direct cascade $\mathcal{T}_{bb}(Q,K)$ gives a negative contribution (up to $k \simeq 20$ in the TG run and larger wave numbers for the ABC case), indicating that each magnetic shell K gives locally more energy to smaller scales than what it receives from the larger scales. This is compensated by the energy injected by the velocity field through the transfer $\mathcal{T}_{ub}$.

B. Saturation of the dynamo

In this section we discuss the evolution of the transfer function for the TG run as the dynamo approaches the nonlinear saturation. The ABC run shows similar features except for a slow growth of the magnetic field at $K=1$, which finally dominates the magnetic energy. The transfer of magnetic energy at the large scales in this case has been studied in [9]. For details of the transfer in the final state reached by the two simulations, we refer the reader to paper I.

Figure 13 shows the $\mathcal{T}_{ub}$ transfer at $K=20$ as a function of

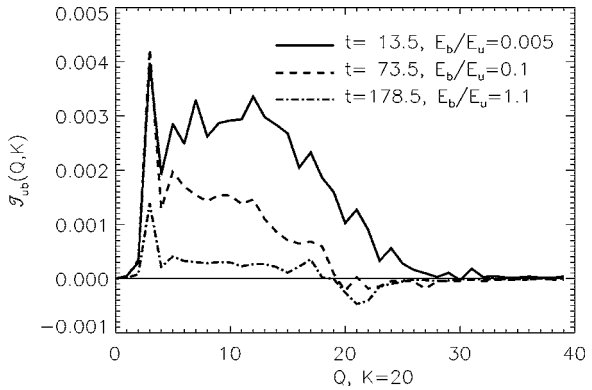

FIG. 13. Transfer function from the kinetic energy at Q to the magnetic energy at $K=20$ for three different times as the magnetic field approaches saturation in the TG run.

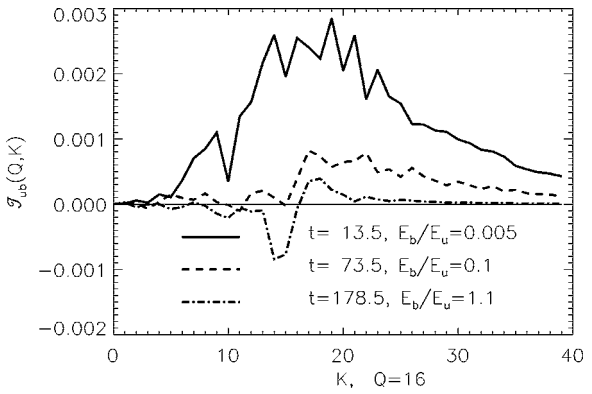

FIG. 14. Transfer function from the kinetic energy at $Q=16$ to the magnetic energy at K for three different times as the magnetic field approaches saturation in the TG run.

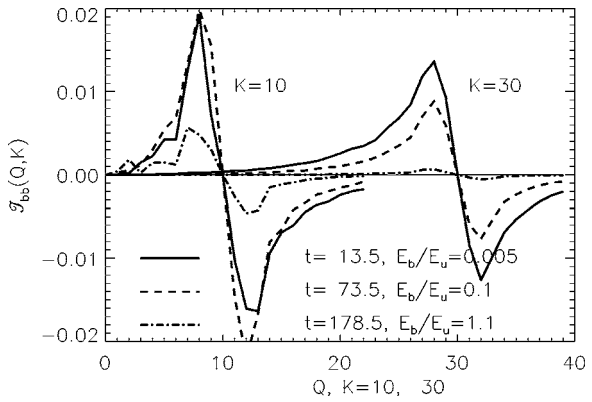

FIG. 15. Transfer of magnetic energy at shell Q to shell K (for $K=10$ and $K=20$) for three different times as the magnetic field approaches saturation in the TG run.

time as the nonlinear saturation takes place. Each transfer has been normalized by the total magnetic energy at that time. The transfer at $t=13.5$ corresponds to the kinematic regime. At $t=73.5$, the small-scale magnetic field saturates and stops growing (see [28]). The velocity field turbulent fluctuations are partially quenched, and the kinetic energy at small scales is reduced. This suppression of turbulence by the magnetic field has been previously observed [9,28], and as a result the transfer of energy to the magnetic field at wave number K from the velocity field between $3<Q\lesssim K$ is also strongly reduced. However, the large-scale velocity field at $Q=3$ keeps transferring energy to the magnetic field. In this stage, the large-scale magnetic field keeps growing until the large scales are dominated by magnetic energy and suppress even more the turbulent fluctuations. At $t=178.5$, the system has finally reached the steady state. The magnetic field at each shell K is sustained by both the large-scale flow and the turbulent fluctuations, but now the amplitude at all scales has been reduced due to the Lorentz force. Note also that the transfer at scales $Q\gtrsim K$ is now negative, pointing to the fact that the magnetic energy is feeding the velocity field at small scales.

In Fig. 14, we show the transfer $\mathcal{T}_{ub}(Q,K)$ for a fixed velocity wave number $Q=16$ for the same times as in Fig. 13. Again, the transfers have been normalized by the total magnetic energy at each time. In the kinematic regime, the velocity field at $Q=16$ gives energy (positive transfer) to the magnetic field at all scales. When the small-scale magnetic field saturates ($t=73.5$) the velocity field at $Q=16$ gives energy only to magnetic shells with $K\geqslant Q$ and modes with $K<Q$ receive almost no energy. This regime corresponds to the case where the magnetic field at small scales has saturated and its energy is sustained by the dynamo without further amplification. The large-scale field keeps growing, mostly fed by the large-scale flow at $Q=3$ as previously discussed. Finally, in the saturated regime ($t=178.5$) the magnetic field at $Q=16$ receives energy from all kinetic shells Q with $K\geqslant Q$, while it gives energy (negative transfer) to all kinetic shells with $K<Q$.

Finally, in Fig. 15 we show the transfer of magnetic to magnetic energy $\mathcal{T}_{bb}$ as a function of time. The local transfer between magnetic shells is not changing as much as $\mathcal{T}_{ub}$ as the dynamo saturates, except for a change in the amplitude. The amplitude is decreasing as saturation is approached, an effect that appears first in the small scales. We note that the role of the local direct cascade $\mathcal{T}_{bb}$ becomes more dominant when compared with the $\mathcal{T}_{bb}$ term as saturation is approached [25].

IV. DISCUSSION

In this work, the transfer of energy from the different scales of the velocity field to the different scales of the magnetic field has been studied. We now give a brief summary of our most important results and discuss the implications for dynamo theory.

It has been shown that the magnetic field grows as the result of a complex interaction between large and small scales. Both large and small scales of the flow give a contribution to the dynamo. The amplification of the large-scale magnetic field during the kinematic regime is due to the large-scale flow (large-scale dynamo). At smaller scales, most of the injection of energy from the velocity field during the kinematic regime is due to the turbulent fluctuations of the velocity field (small scale dynamo). A competing mechanism for the amplification of the magnetic field at the small scales is the cascade of magnetic field energy from the large scales to the small scales that is also transferring energy to the small scales. The rate that energy is transfered to the small scales through the cascading process is smaller than the rate that the velocity field is injecting energy at the small scales for a finite range of wave numbers. For sufficiently small scales (close to the scale at which the peak of the magnetic energy spectrum is reached), the cascading term becomes larger than the small-scale dynamo term.

The results in this paper and the formalism used help us understand and classify the dynamo processes involved in the amplification of the magnetic field. In this formalism, we were able to measure and compare each component in the dynamo process that is involved in the amplification of the magnetic field in both small and large scales. Therefore, we can distinguish between different dynamos based on whether the cascading terms dominate over the injection terms in the

small scales and on whether the turbulent fluctuations are more dominant for the generation of the magnetic field when compared with the input from the large scale flow. Of course, this is not the only possible distinction that can be made between dynamos; however, it is an important step towards classifying dynamos in the presence of both a large-scale flow and turbulent fluctuations.

Finally we would like to note that the investigation of the growth of a large-scale magnetic field with enough scale separation between the forced scale and the domain size is required to study processes such as the dynamo α effect and the inverse cascade of magnetic helicity. A similar analysis will be performed in this context in future works.

ACKNOWLEDGMENTS

The authors are grateful to J. Herring for valuable discussions and his careful reading of this document. Computer time was provided by NCAR and Pittsburgh Supercomputing Center. NSF Grant No. CMG-0327888 at NCAR supported this work in part and is gratefully acknowledged.

[1] H. K. Moffatt, *Magnetic Field Generation in Electrically Conducting Fluids* (Cambridge University Press, Cambridge, England, 1978).
[2] M. Dikpati and P. Charbonneau, Astrophys. J. **518**, 508 (1999).
[3] F. Cattaneo, Astrophys. J. Lett. **515**, L39 (1999).
[4] S. I. Vainshtein and Y. B. Zeldovich, Sov. Phys. Usp. **15**, 159 (1972).
[5] M. Steenbeck, F. Krause, and K.-H. Raedler, Z. Naturforsch. A **21**, 369 (1966).
[6] F. Krause and K.-H. Raedler, *Mean-field Magnetohydrodynamics and Dynamo Theory* (Pergamon Press, New York, 1980).
[7] A. Pouquet, U. Frisch, and J. Léorat, J. Fluid Mech. **77**, 321 (1976).
[8] M. Meneguzzi, U. Frisch, and A. Pouquet, Phys. Rev. Lett. **47**, 1060 (1981).
[9] A. Brandenburg, Astrophys. J. **550**, 824 (2001).
[10] D. O. Gómez and P. D. Mininni, Nonlinear Processes Geophys. **11**, 619 (2004).
[11] A. Gilbert, U. Frisch, and A. Pouquet, Geophys. Astrophys. Fluid Dyn. **42**, 151 (1988).
[12] C. Nore, M. E. Brachet, H. Politano, and A. Pouquet, Phys. Plasmas **4**, 1 (1997).
[13] V. Urpin, Phys. Rev. E **65**, 026301 (2002).
[14] U. Geppert and M. Rheinhardt, Astron. Astrophys. **392**, 1015 (2002).
[15] A. P. Kazanstev, Sov. Phys. JETP **26**, 1031 (1968).
[16] Y. B. Zeldovich, A. A. Ruzmaikin, and D. D. Sokoloff, *Magnetic Fields in Astrophysics* (Gordon and Breach, New York, 1983).
[17] A. A. Schekochihin, S. Boldyrev, and R. M. Kulsrud, Astrophys. J. **567**, 828 (2002).
[18] N. E. L. Haugen, A. Brandenburg, and W. Dobler, Astrophys. J. Lett. **597**, L141 (2003).
[19] A. A. Schekochihin, S. C. Cowley, S. F. Taylor, J. L. Maron, and J. C. McWilliams, Astrophys. J. **612**, 276 (2004).
[20] S. Boldyrev, F. Cattaneo, and R. Rosner, e-print astro-ph/0504588.
[21] G. K. Batchelor, Proc. R. Soc. London, Ser. A **201**, 405 (1950).
[22] A. A. Schekochihin, S. C. Cowley, J. L. Maron, and J. C. McWilliams, Phys. Rev. Lett. **92**, 054502 (2004).
[23] Y. Ponty, P. D. Mininni, D. C. Montgomery, J.-F. Pinton, H. Politano, and A. Pouquet, Phys. Rev. Lett. **94**, 164502 (2005).
[24] K. Subramanian, Phys. Rev. Lett. **83**, 2957 (1999).
[25] A. Alexakis, P. D. Mininni, and A. Pouquet, preceeding paper, Phys. Rev. E **72**, 046301 (2000).
[26] G. Dar, M. Verma, and V. Eswaran, Physica D **157**, 207 (2001).
[27] O. Debliquy, M. Verma, and D. Carati, Phys. Plasmas **12**, 042309 (2005).
[28] P. D. Mininni, Y. Ponty, D. C. Montgomery, J.-F. Pinton, H. Politano, and A. Pouquet, Astrophys. J. **626** 853 (2005).
[29] P. D. Mininni, D. C. Montgomery, and A. Pouquet, Phys. Rev. E **71**, 046304 (2005).